A Hot Spot Model for Black Hole QPOs

Jeremy Schnittman* and Edmund Bertschinger*

*MIT Department of Physics, 77 Massachusetts Avenue, Cambridge, MA 02139

Abstract. In at least two black hole binary systems, the Rossi X-Ray Timing Explorer has detected high frequency quasi-periodic oscillations (HFQPOs) with a 2:3 frequency commensurability. We propose a simple hot spot model to explain the positions, amplitudes, and widths of the HFQPO peaks. Using the exact geodesic equations for the Kerr metric, we calculate the trajectories of massive test particles, which are treated as isotropic, monochromatic emitters in their rest frames. By varying the hot spot parameters, we are able to explain the different features observed in "Type A" and "Type B" QPOs from XTE J1550-564. In the context of this model, the observed power spectra allow us to infer values for the black hole mass and angular momentum, and also constrain the parameters of the model.

INTRODUCTION

One of the most exciting results from the Rossi X-Ray Timing Explorer was the discovery of high frequency quasi-periodic oscillations from neutron star and black hole binaries [1, 2, 3]. For black hole systems, these HFQPOs are observed repeatedly at more or less constant frequencies, and in a few cases with integer ratios [4]. These measurements give the exciting prospect of determining a black hole's mass and spin, as well as testing general relativity in the strong-field regime. To quantitatively interpret these observations in the context of the space-time behavior near the black hole inner-most stable circular orbit (ISCO), we have developed a ray-tracing code to model the X-ray light curve from a collection of "hot spots," small regions of excess emission moving on geodesic orbits. The methods and basic results of this code are described in detail in [5].

This hot spot model is motivated by the similarity between the QPO frequencies and the black hole coordinate frequencies near the ISCO [6, 7] as well as the suggestion of a resonance leading to integer commensurabilities between these coordinate frequencies [8, 9]. Stella and Vietri [7] investigated primarily the QPO frequency pairs found in LMXBs with a neutron star accretor, but their basic methods can be applied to black hole systems as well. Perhaps the most powerful feature of this hot spot model is the facility with which it can be developed and extended to more general accretion disk geometries. For example, our ray-tracing code could be used in conjunction with a 3D MHD calculation of the accretion disk to simulate the time-dependent X-ray flux and spectrum from such a disk.

RAY TRACING IN THE KERR METRIC

While the details of the ray tracing algorithm are presented in full in [5], we give here a short summary of our methods. We begin by dividing the image plane into regularly spaced "pixels" of equal solid angle in the observer's frame, each corresponding to a single ray. Following the sample rays backward in time, we calculate the original position and direction that a photon emitted from the disk would require in order to arrive at the appropriate position in the detector. The gravitational lensing and magnification of emission from the plane of the accretion disk is performed automatically by the geodesic integration of these evenly spaced photon trajectories, so that high magnification occurs in regions where nearby points in the disk are projected to points with large separation in the image plane. To model the time-varying emission from the disk, each photon path is marked with the time delay along the path from the observer to the emission point in the disk.

To integrate the geodesic trajectories of photons or massive particles, we use a Hamiltonian formalism that takes advantage of certain conserved quantities in the dynamics: the energy, angular momentum, and mass of each particle. By eliminating the energy ($E = -p_t$) from the Hamiltonian, we can use the conjugate coordinate t as the integration variable, thus reducing the problem from eight phase space dimensions to six. Another integral of the motion, Carter's constant Q [10], is not explicitly conserved in our equations, but rather is used as an independent check for the accuracy of the numerics. The resulting equations of motion do not contain any sign ambiguities from turning points in the orbits, as are introduced by many classical treatments of the geodesic equations in the Kerr metric.

The photon trajectories are integrated backward in time from the image plane oriented at some inclination angle i with respect to the axis of rotation for the black hole, where $i = 0°$ corresponds to a face-on view of the disk and $i = 90°$ is an edge-on view. The accretion disk is confined to a finite region of latitude and is assumed to be oriented normal to the rotation axis. The photons terminate either at the event horizon or pass through the surfaces of colatitude $\theta = \text{const}$. As trajectories pass through the disk, the photon's position and momentum (x^μ, p_μ) are recorded for each plane intersection in order to later reconstruct an image of the disk. The results of this paper are based primarily on flat disks with simple hot spot perturbations, yet with the computational methods described above, arbitrary disk geometries and emissivity/opacity models can be simulated as well.

HOT SPOT EMISSION

Given the map from the accretion disk to the image plane, with each photon bundle labeled with a distinct 4-momentum and time delay, we can reconstruct time-varying images of the disk based on time-dependent emission models. The simplest model we consider is a single region of isotropic, monochromatic emission following a geodesic trajectory: the "hot spot" model [6, 7]. We treat the hot spot as a small region of the disk with additional emissivity chosen to have a Gaussian distribution in local Cartesian space. We typically take $R_{\rm spot} = 0.25 - 0.5M$, but find the normalized light curves and QPO power spectra to be independent of spot size and shape.

By definition the hot spot will have a higher temperature or density and thus greater emissivity than the background disk, adding a small modulation to the total flux. RXTE observations find the HFQPO X-ray modulations to have typical amplitudes of 1-5% of the mean flux during the outburst [4]. Assuming a Shakura-Sunyaev type disk [11] with steady-state emissivity $g(r) \propto r^{-2}$ and a similar scaling for the hot spot emission, we find that small hot spots with overbrightness of $\approx 100\%$ (consistent with 3D MHD calculations [12]) are easily capable of creating X-ray modulations on the order of 1% rms.

As the disk inclination increases, the light curve goes from nearly sinusoidal to being sharply peaked by special relativistic beaming. Thus the shape of a QPO light curve may be used to determine the disk inclination. Since current observations cannot resolve the X-ray signal over individual periods as short as 3-5 ms, instead the Fourier power spectrum can be used to identify the harmonic features of the light curve over many orbits. Disks with higher inclinations will give more power in the higher harmonic frequencies, due to the "lighthouse" effect, as

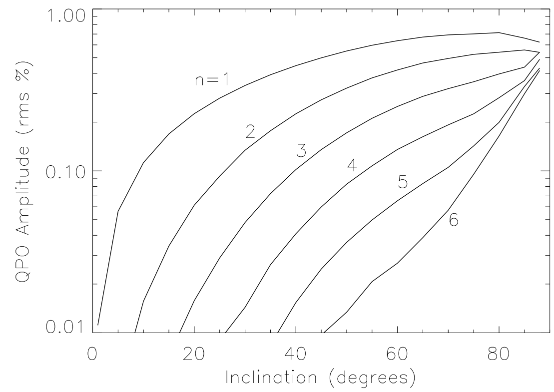

FIGURE 1. Fourier amplitude $a_n(\text{rms})$ in higher harmonic frequencies $\nu_n = n\nu_\phi$ as a function of orbital inclination to the observer, normalized as in Eqn. 2. The hot spot has size $R_{\rm spot} = 0.5M$, an overbrightness factor of 100%, and is in a circular orbit at $R_{\rm ISCO}$ around a Schwarzschild black hole.

the hot spot shoots a high-power beam of photons toward the observer once per orbit, approximating a periodic delta-function in time.

Figure 1 shows the quantitative dependence of harmonic power on disk inclination for a hot spot orbiting at the ISCO of a Schwarzschild black hole. Predictably, as the inclination increases, we see that both the absolute and relative amplitudes of the higher harmonics increase, almost to the limit of a periodic delta-function when $i \to 90°$. Again, we find very little dependence of the harmonic structure on hot spot size or shape, as long as the total emission of the spot relative to the disk is constant. Here we have normalized the rms amplitudes to the background flux from the disk with a hot spot overbrightness of 100%. For a signal $I(t)$ with Fourier components a_n:

$$I(t) = \sum_{n=0}^{\infty} a_n \cos(2\pi nt), \tag{1}$$

we define the rms amplitude $a_n(\text{rms})$ in each mode $n > 0$ as

$$a_n(\text{rms}) \equiv \frac{a_n}{\sqrt{2a_0}}. \tag{2}$$

With this normalization, the total rms can be conveniently written

$$\text{rms} = \sqrt{\sum a_n^2(\text{rms})}. \tag{3}$$

FITTING QPO DATA

The high frequency QPOs observed with RXTE can be interpreted in the context of the hot spot model by matching the model parameters to the features of the QPO power spectrum, particularly the locations, amplitudes, and widths of the peaks. This problem of fitting a power spectrum to the parameters of a multi-dimensional model is analogous to the spectacular successes that have recently been made in observing and interpreting the perturbations in the cosmological microwave background (CMB). Like the CMB power spectrum, the features of the QPO power spectrum often can be isolated and fitted to one or two of the model parameters at a time. We approach this problem in the systematic step-by-step procedure outlined below, using the example of the Type A QPOs from XTE J1550-564 [4] as case study.

First, we match the frequencies of the QPO peaks to the coordinate frequencies of specific geodesic orbits around a black hole in order to determine the black hole mass and angular momentum. The 2:3 frequency commensurability of the two major peaks (and possibly 2:3:4 in some observations) directs our attention to orbits with radial and azimuthal frequencies with a ratio of $\nu_r : \nu_\phi$ =1:3. The choice of the 1:3 ratio instead of 2:3 gives the appropriate relative power in the two peaks-a major peak at the fundamental azimuthal orbital frequency with additional power in the sidebands at $\nu = \nu_\phi \pm \nu_r$. Conversely, a ratio of 2:3 in the coordinate frequencies would actually give a 1:3:5 ratio in the major power spectrum peaks. For any value of the black hole spin $0 \le a/M \le 1$, there exists a special radius where nearly circular orbits will have the appropriate 1:3 ratio in coordinate frequencies. Then by scaling the black hole mass, we can match the actual peak locations to the data, giving a one-dimensional degeneracy in mass-spin parameter space.

This degeneracy could be broken by identifying the low frequency QPOs with the Lens-Thirring precessional frequency at the same special radius. However, this association is still quite speculative and has difficulty explaining the large rms amplitude of the LFQPOs. For the present, we will constrain our model to a region of this degeneracy limited by the independent black hole mass determination of radial velocity measurements, giving $8.5 < M/M_\odot < 11.5$ [13]. For the QPO peaks at 184 Hz and 276 Hz in XTE J1550, we choose $M = 10.3M_\odot$ and $a/M = 0.5$, giving a geodesic orbital radius of $r_0 = 4.89M$, somewhat outside the ISCO at $R_{\rm ISCO} = 4.23M$.

Next, we match the total rms amplitudes in the two major peaks by selecting an average hot spot overbrightness of 100% and radius $R_{\rm spot} = 0.35M$. The disk inclination is independently determined to be $i \approx 70°$ [13]. As explained in the previous section, this relatively high inclination should produce significant power in many of the higher harmonics at integer multiples of the fundamental frequency $\nu = n\nu_\phi$. These harmonics lie well within the sensitivity range of RXTE, yet are not detected with such high amplitudes. Instead, we find that by shearing the hot spot into an arc of finite length in azimuth, the power at higher frequencies is strongly damped, due to the countering of the lighthouse effect when the emission region is spread out over a larger portion of the orbit [5]. An arc length of 180° gives the appropriate amount of power around 184 Hz and 276 Hz while also successfully decreasing the power at higher frequencies.

The relative power in the two major peaks is primarily determined by the eccentricity of the geodesic orbit, as well as the arc length of the hot spot emission region. For the Type A QPOs, even the modest eccentricity of 0.11 is sufficient to produce significant power in the "sideband" at 184 Hz. Even the Type B QPOs, where the peak at 184 Hz is stronger than the fundamental peak at 276 Hz, can be explained easily in the context of the hot spot model by shearing the arc almost to a ring-shaped perturbation with arc length 330°. For both cases, it is not obvious why there should be such a small amount of predicted power at $\nu_\phi + \nu_r$ =368 Hz, further advocating the necessity of a full ray-tracing algorithm, as opposed to simple analysis of the coordinate frequencies.

Up to this point, all of the ingredients of the hot spot model combine to produce a power spectrum with a series of discrete peaks describing a purely periodic light curve. In order to understand the significant broadening of the peaks (and thus the term *quasi*-periodic), we generalize the hot spot model by replacing a single spot orbiting indefinitely on a single trajectory by a collection of hot spots that are continually created and destroyed with random phase along their orbits. Each hot spot lifetime t has an exponential distribution function $f(t) \propto \exp(-t/T)$ with a probability $P = dt/T$ of being "destroyed" during each time step dt. When one hot spot is destroyed, a new hot spot is created with the same r_0 but with random orbital phase. The effect is to spread each delta-function feature in the periodic power spectrum into a Lorentzian peak with FWHM $\propto 1/T$. With this multiple hot spot model, the power spectrum from XTE J1550 is closely matched by setting the typical lifetime $T = 15$ ms, or approximately four orbits in azimuth.

The summary of these best-fit results is shown in Table 1, and the corresponding power spectrum (calculated from a Monte-Carlo simulation of the light curve over many hot spot lifetimes) is shown in Figure 2. The solid curve is the best fit of a collection of Lorentzians to the simulated data, included a small background counting noise level with a Poisson distribution. Again, the analogy to the CMB data is evident, and just like with the CMB, each successive advance in instrumentation brings us closer to a precise determination of the model parameters. However, for the QPOs, in addition to the power spectrum, there is also significant information in the light curve phase, if we can achieve the necessary sensitivity to resolve the signal in the time domain. This phase information promises to ultimately help in distinguishing

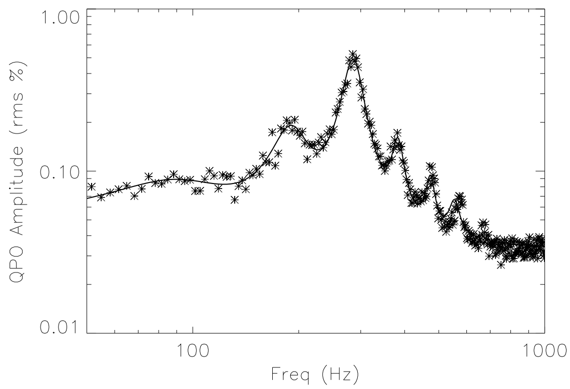

FIGURE 2. Simulated QPO power spectrum for a set of model parameters described in Table 1, selected to fit the spectra of Type A QPOs from XTE J1550-564. The solid line is a fit to the simulated data with a series of Lorentzian peaks.

TABLE 1. Hot spot model parameters for Type A HFQPOs from XTE J1550-564

Parameter	Value
BH mass	$10.3M_{\odot}$
BH spin a/M	0.5
disk inclination	70°
geodesic r_0	$4.89M$
$R_{\rm spot}$	$0.35M$
eccentricity	0.11
arc length	180°
overbrightness	100%
hot spot Lifetime T (4 orbits)	15 ms
Lorentzian FWHM	45 Hz

between the various proposed explanations of the cause of the black hole QPOs.

We have also investigated the effect of various distributions in orbital eccentricity, overbrightness, and the number of simultaneous hot spots at any time. Interestingly, we find that the QPO power spectrum is dependent only on the *average* eccentricity and overbrightness, and is not sensitive to the actual shape of the distribution. Similarly, the power spectrum is independent of the number of different hot spots in existence at any given time, sensitive only to the average lifetime of each hot spot.

One major remaining issue with the hot spot model is the preferred location of the geodesic that gives rise to 1:3 coordinate frequencies. Why should the orbital frequencies favor integer ratios, and why should the preferred ratio be 1:3 and not 1:2 or 1:4? It is possible that detailed radiation-hydrodynamic calculations with full general relativity will be required to answer this question. Perhaps the non-circular orbits can only survive along closed orbits such as these to somehow avoid destructive intersections. For now, we are forced to leave this as an open question unanswered by the geodesic hot spot model.

Yet with the computational framework developed above, these questions can be answered by modeling a whole collection of hot spots and arcs continually forming and evolving in shape and emissivity. The particular physical parameters for these hot spots can be derived from published MHD calculations such as [12]. With the basic ray-tracing and radiation transport methods in place, it should be possible to use our code as a "post-processor" to analyze the results of these 3D simulations to simulate X-ray light curves and spectra from a realistic accretion disk.

A final piece of the black hole QPO puzzle is the spectral behavior of the source during outburst. Remillard et al. [4] have shown there is a large range of X-ray fluxes with different relative contributions from a power-law component and a disk bolometric component. These relative and absolute fluxes seem to be correlated with the amount of power in both the LFQPOs and the HFQPOs. Future work on 3-dimensional disks and more detailed radiation transfer models should give us important insights into understanding this spectral behavior and its relation to the QPO power.

ACKNOWLEDGMENTS

We would like to thank Ron Remillard for many helpful discussions. This work was supported by NASA grant NAG5-13306.

REFERENCES

1. Strohmayer, T. E. et al. 1996, ApJ, 469, L9
2. Strohmayer, T. E. 2001, ApJ, 552, L49
3. Lamb, F. K. 2002, in *X-ray Binaries and Gamma-Ray Bursts*, ed. E. P. J. van den Heuvel (San Francisco: Astronomy Society of the Pacific)
4. Remillard, R. A. et al. 2002, ApJ, 580, 1030
5. Schnittman, J. D., & Bertschinger, E. 2003, submitted to ApJ (astro-ph/0309458)
6. Stella, L., & Vietri, M. 1998, ApJ, 492, L59
7. Stella, L., & Vietri, M. 1999, Phys. Rev. Lett., 82, 17
8. Kluzniak, W., & Abramowicz, M. A. 2001, preprint (astro-ph/0105057)
9. Kluzniak, W., & Abramowicz, M. A. 2002, preprint (astro-ph/0206063)
10. Carter, B. 1968, Phys. Rev. Lett. 26, 331
11. Shakura, N. I., & Sunyaev, R. A. 1973, Astron. Astrophys., 24, 337
12. Hawley, J. F., & Krolik, J. H. 2001, ApJ, 548, 348
13. Orosz, J. A. et al. 2002, ApJ, 568, 845